

PERFORMANCE ANALYSIS OF BAND-LIMITED GENERALIZED MULTICARRIER CDMA SYSTEMS

Besma Smida and Sofiène Affes

INRS-EMT, Université du Québec, Montréal, Québec, H5A 1K6, Canada
E-mails: {smida,affes}@emt.inrs.ca

ABSTRACT

In this paper, we extend the investigation of the generalized MC-CDMA system by considering a practical band-limited chip waveform, namely, a square-root raised cosine waveform. The analysis is based on the standard Gaussian approximation. The effects of the chip waveform and the spacing between two adjacent subcarriers on the interference level and on the average BER have been evaluated. The results show that for a given subcarrier spacing between two adjacent subcarriers, there exists a corresponding best choice of the chip waveform. In addition, they suggest that MT-CDMA has the optimum spacing between subcarriers and achieves the best BER performance.

1. INTRODUCTION

Recently, a number of multi-carrier code-division multiple access (Multicarrier CDMA) systems have been proposed as an alternative to the classical direct-sequence CDMA (DS-CDMA). Among these systems, multi-carrier direct-sequence CDMA (MC-DS-CDMA) and multitone CDMA (MT-CDMA) combine time-domain spreading and multicarrier modulation, as opposed to the combination of frequency-domain spreading and multicarrier modulation of other systems [1]. MC-DS-CDMA and MT-CDMA can be unified in a family of generalized MC-DS-CDMA transceivers, defined in [2], using a range of frequency spacings, parameterized by λ , between two adjacent subcarriers. In this paper we adopt this general view and simply refer to it as MC-CDMA in the remainder of the paper unless otherwise required.

The multiple access interference (MAI) and the inter-symbol interference (ISI), which are inherited from conventional DS-CDMA, affect likewise the performance of MC-CDMA systems. In addition, MC-CDMA capacity is limited by the inter-carrier interference (ICI) due to the use of multicarrier modulation. The chip waveform has been noted to be an important system parameter for conventional DS-CDMA. The effect of both time-limited and band-limited

waveforms on MAI level in DS-CDMA has been investigated [3][4]. However, for all the MC-CDMA systems found in the literature, a time-limited waveform is generally employed [2][5][6][7]. All these papers assumed that the chip waveform is time limited to $[0, T_c]$, where T_c is the chip duration and that the system occupies an infinite bandwidth so that the chip waveform experiences no distortion during transmission. A practical system, in contrast, always involves band-limitation filtering to restrict out-of-band radiation. For example, wideband CDMA (W-CDMA) employs square-root raised cosine pulse shaping with a rolloff factor of $\beta = 0.22$. Band-limitation filtering causes the chip waveforms to disperse over the time axis and overlap one another, which would violate the assumption of the above-referenced papers. Almost no paper addressed the performance analysis of an MC-CDMA system in a band-limited-chip scenario. The difficulty lies in the calculation of the variance of the interference. The exception is in [8], where recently the use of several band-limited chip waveforms for MC-DS-CDMA systems (a subclass of MC-CDMA) was considered.

In this paper, we derive the interference variance of MC-CDMA (including MC-DS-CDMA and MT-CDMA) with a *band-limited* square-root raised cosine (square RRC) waveform using a frequency-domain approach [9]. This analysis, which is based on the standard Gaussian approximation, allows us to evaluate the impact of some system parameters, such as the chip waveform and the spacing between two adjacent subcarriers, on the interference level and on the average bit error rate (BER) of the MC-CDMA system.

2. SYSTEM MODEL AND ASSUMPTIONS

2.1. MC-CDMA Transmitter

We consider the uplink of an asynchronous multi-cellular multicarrier CDMA system with U in-cell active users. For the sake of simplicity, we assume that all users use the same subcarriers and transmit with the same modulation at the same rate. The input information sequence of the u -th user is first converted into K parallel data sequences

*: Work supported by a Canada Research Chair in High-Speed Wireless Communications and the Strategic Project Program of NSERC.

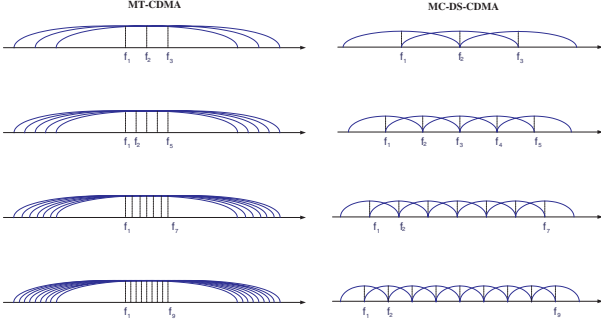


Fig. 1. Different configurations of MT-CDMA and MC-DS-CDMA within the same bandwidth.

$b_{1,n}^u, \dots, b_{K,n}^u$ where n is the time index. The data $b_{k,n}^u$ is \mathcal{M} -PSK modulated and encoded at rate $1/T_{MC}$, where $T_{MC} = K \times T$ is the symbol duration after serial/parallel (S/P) conversion. The resulting S/P converter output is then spread with a random spreading code $c_n^u(t)$ at a rate $1/T_c$. The spreading factor, defined as the ratio between the chip rate and the symbol rate is $L = \frac{T_{MC}}{T_c}$. We write the spreading-code segment over the n -th period T_{MC} as:

$$c_n^u(t) = \sum_{l=0}^{L-1} c_{l,n}^u \phi(t - lT_c - nT_{MC}), \quad (1)$$

where $c_{l,n}^u = \pm 1$ for $l = 0, \dots, L-1$, is a random sequence of length L and $\phi(t)$ is the chip pulse. We consider square-root raised cosine chip pulses with rolloff factor β . Closed-loop power control is taken into account at the transmitter by the amplification factor $a^u(t)$. All the data are then modulated in baseband by the inverse discrete Fourier transform (IDFT) and summed to obtain the multi-carrier signal. Finally the signal is transmitted after radio-frequency up-conversion. The transmitted signal of the u -th user is given by:

$$s^u(t) = \sum_{k=1}^K \sum_{n=-\infty}^{\infty} a^u(t) b_{k,n}^u c_n^u(t) e^{j2\pi f_k t}. \quad (2)$$

The modulated subcarriers are orthogonal over the symbol duration T_{MC} . The frequency corresponding to the k -th subcarrier is $f_k = f_p + \lambda \times k/T_{MC}$, where f_p is the fundamental carrier frequency. The transmitter belongs to the family of MT-CDMA if λ is set to 1, and to the class of MC-DS-CDMA if λ is set to L (see resulting signal spectra in Fig. 1).

For a fair comparison among different configurations of MC-CDMA, the bandwidth and the data rate should be the same. We choose as a reference the DS-CDMA ($K = 1$) system with spreading factor L_1 and frequency selective fading with P_1 propagation paths. Then, the total transmitted bandwidth of MC-CDMA BW , which is equal the total

null-to-null bandwidth of the reference DS-CDMA system, is:

$$BW = \frac{2L_1}{T} = \frac{(K-1)\lambda}{T_{MC}} + \frac{(1+\beta)}{T_c}. \quad (3)$$

Multiplying both sides of the above equation by the symbol duration T_{MC} , and taking into account that $T_{MC} = LT_c$ as well as that $T_{MC} = KT$, the processing gain L of the subcarrier signal can be expressed as:

$$L = \frac{2L_1 K}{1+\beta} - \frac{(K-1)\lambda}{1+\beta}, \quad (4)$$

which implies that, for a given total system bandwidth of BW and a given number of subcarriers K , L decreases as λ increases.

2.2. Channel Model

We consider transmission to M receiving antennas. The channel is assumed to be a slowly varying frequency selective Rayleigh channel with delay spread $\Delta\tau$. Then, the number of resolvable paths, P , associated with each configuration of MC-CDMA is given by $P = \lfloor \Delta\tau/T_c \rfloor + 1$, where $\lfloor x \rfloor$ is the largest integer not exceeding x . The number of resolvable path, P_1 , in the case of the reference DS-CDMA is given by $P_1 = \lfloor \Delta\tau/(T/L_1) \rfloor + 1$. Multiplying both sides of Eq. (3) by $\Delta\tau$, we obtain that P and P_1 are related by

$$P \approx \lfloor \frac{2L(P_1 - 1)}{(1+\beta)L + (K-1)\lambda} \rfloor + 1. \quad (5)$$

We note here that the large-scale path-loss that includes free-space path-loss and shadowing is the same for all subcarriers. Moreover the number of resolvable paths P and their propagation time-delays τ_1, \dots, τ_P depend on the reflecting objects and scatterers and, therefore, can be assumed equal for all subcarriers [10]. We assume that the received channel multipath components across the M antennas are independent. The M -dimensional complex low-pass equivalent vector representation of the impulse response experienced by subcarrier k of the u -th user, for a receiver equipped with M antennas, is:

$$H_k^u(t) = \frac{\rho^u(t)}{(r^u)^e(t)} \sum_{p=1}^P \mathcal{G}_{k,p}^u(t) \delta(t - \tau_p^u(t)), \quad (6)$$

where $\rho^u(t)$ and $(r^u)^e(t)$ model the effects of shadowing and path loss, respectively, $r(t)$ is the distance from the user to the base-station and e is the path-loss exponent. The M -dimensional complex vector $\mathcal{G}_{k,p}^u(t)$ denotes the fading and the array response from the user to the antenna elements of the receiver and $\tau_p^u(t)$ represents the propagation time-delay along the p -th path.

2.3. Received Signal

For a multi-cellular MC-CDMA system with U in-cell users and K carriers, the received signal is the superposition of signals from all users and all subcarriers. Hence the M -dimensional observation vector received, after downconversion, by the antenna array can be expressed as follows:

$$\begin{aligned} X(t) &= \sum_{u=1}^U \sum_{k=1}^K \sum_{n=-\infty}^{\infty} H_k^u(t) \otimes a^u(t) b_{k,n}^u c_n^u(t) e^{j2\pi f_k t} \\ &\quad + N(t), \\ &= \sum_{u=1}^U \sum_{k=1}^K \sum_{n=-\infty}^{\infty} X_{k,n}^u(t) + N(t), \end{aligned} \quad (7)$$

where \otimes denotes time convolution. The noise term $N(t)$ includes the thermal noise received at the antennas as well as the out-cell interference. The contribution $X_{k,n}^u(t)$ of the n -th data symbol over the k -th carrier of user u to the received vector $X(t)$ is given by:

$$\begin{aligned} X_{k,n}^u(t) &= H_k^u(t) \otimes a^u(t) b_{k,n}^u c_n^u(t) e^{j2\pi f_k t}, \\ &= \psi_k^u(t) b_{k,n}^u \sum_{p=1}^P G_{k,p}^u(t) \epsilon_{k,p}^u(t) c_n^u(t - \tau_p^u) \\ &\quad \times e^{j2\pi f_k (t - \tau_p^u)}. \end{aligned} \quad (8)$$

Along the p -th path, $G_{k,p}^u = \mathcal{G}_{k,p}^u (\sqrt{M} / \|\mathcal{G}_{k,p}^u\|)$ is the propagation vector over the k -th subcarrier of the u -th user with norm \sqrt{M} and $(\epsilon_{k,p}^u)^2(t) = \|\mathcal{G}_{k,p}^u\|^2 / \sum_{p=1}^P \|\mathcal{G}_{k,p}^u\|^2$ is the fraction of the total received power on the k -th subcarrier of user u :

$$\psi_k^u(t)^2 = \left(\frac{\rho}{(r^u)^e(t)} \right)^2 (a^u)^2(t) \sum_{p=1}^P \frac{\|\mathcal{G}_{k,p}^u\|^2}{M}. \quad (9)$$

3. PERFORMANCE ANALYSIS

In this section, we analyze the statistics of the interference. Without loss of generality, let us focus on the detection of the n -th symbol carried by the k -th carrier of the desired user assigned index $u \in \{1, \dots, U\}$, i.e., $b_{k,n}^u$. We define the post-correlated observation vector over a time-interval $[0, T_{MC}]$ as:

$$\begin{aligned} Z_{k,n}^u(t) &= \frac{1}{T_{MC}} \int_0^{T_{MC}} \sum_{u'=1}^U \sum_{k'=1}^K \sum_{n'=-\infty}^{\infty} X_{k',n'}^{u'}(nT_{MC} + t + t') \\ &\quad \times c_n^u(t' + nT_{MC}) e^{-j2\pi f_k (t' + nT_{MC})} dt' + N_{k,n}^u(t) \\ &= D_{k,n}^u + I + N_{k,n}^u(t), \end{aligned} \quad (10)$$

where $D_{k,n}^u$ is the desired signal. The total interference I includes three types of interference: 1) The multiple access interference I_{MAI} is the interference due to the K carriers from the other in-cell users $u' \neq u$. 2) The inter-carrier interference I_{ICI} is the interference due to the other carriers,

$k' \neq k$, from the same user u . 3) The inter-symbol interference I_{ISI} is the interference due to the same carrier k from the same user u . The noise vector $N_{k,n}^u(t)$ comprises the post-correlation thermal noise (with variance σ_N^2) and the interference due to out-of-cell users. The interference contribution $I_{k'}^{u'}(t)$ of the k' -th carrier of user u' to the received vector is given by Eq. (11) (see next page). We assumed in the development of Eq. (11) above that $\psi_{k'}^{u'}(nT_{MC} + t + t')$, $G_{k',p}^{u'}(nT_{MC} + t + t')$ and $\epsilon_{k',p}^{u'}(nT_{MC} + t + t')$ are constant during the interval $t' \in [0, T_{MC}]$. Having analyzed the interference terms in Eq. (11), let us now consider the statistics of these interference contributions by assuming random spreading sequences and employing the standard Gaussian approximation. We assume here that the interference are Gaussian random variables with zero mean. Hence, we only need to evaluate their variances. By substituting Eq. (1) in Eq. (11) and letting $I_{k',p}^{u'}$ be the average power of the p -th path over the k' -th carrier of the user u' , the variance of the interference $I_{k'}^{u'}(t)$ can be written as:

$$\begin{aligned} \text{Var}[I_{k'}^{u'}(t)] &= \frac{L}{T_{MC}^2} \sum_{p=1}^P I_{k',p}^{u'} T_c^2 E \left\{ \sum_{l=-\infty}^{\infty} |\rho(lT_c - \tau_p^{u'})|^2 \right\}, \\ &= \frac{1}{L} \sum_{p=1}^P I_{k',p}^{u'} \left[\frac{1}{T_c} \int_{-\infty}^{+\infty} |\rho(t)|^2 dt \right], \end{aligned} \quad (12)$$

where $\rho(t)$ is the inter-correlation function between the chip waveform $\phi(t)$ and the out-of-phase chip waveform $\phi(t)e^{-j2\pi(f_{k'} - f_k)(t)}$. If $\phi(t)$ is time-limited, such as the rectangular time-limited impulse, the analysis is preferably carried out in the time domain; while since $\phi(t)$ is band-limited, the frequency domain analysis is preferred. Hence in the frequency domain, the variance of the interference $I_{k'}^{u'}(t)$ can be written as:

$$\text{Var}[I_{k'}^{u'}(t)] = \frac{1}{L} \sum_{p=1}^P I_{k',p}^{u'} \left[\frac{1}{T_c} \int_{-\infty}^{\infty} G(f) G(f - (f_k - f_{k'})) df \right], \quad (13)$$

where $G(f)$ is the Fourier transform of the raised-cosine filter [8]:

$$G(f) = \begin{cases} \frac{T_c}{2}, & 0 \leq |f| \leq \frac{1-\beta}{2T_c} \\ \frac{T_c}{2} + \frac{T_c}{2} \cos \left[\frac{\pi T_c}{\beta} \left(|f| - \frac{1-\beta}{2T_c} \right) \right], & \frac{1-\beta}{2T_c} \leq |f| \leq \frac{1+\beta}{2T_c} \\ 0, & |f| > \frac{1+\beta}{2T_c} \end{cases} \quad (14)$$

After mathematical derivations, we obtain $\zeta(\beta) = \frac{1}{T_c} \int_{-\infty}^{\infty} G^2(f) df$ and $\chi(\beta) = \max_k [\chi_k(\beta)]$, where

$$\begin{aligned} \chi_k(\beta) &= \sum_{\substack{k'=-K \\ k' \neq k}}^K \frac{1}{T_c} \int_{-\infty}^{\infty} G(f) G(f - (f_k - f_{k'})) df \\ &= \sum_{\substack{k'=-K \\ k' \neq k}}^K \vartheta \left(\frac{|k-k'|\lambda}{LT_c} \right) = \sum_{\substack{k'=-K \\ k' \neq k}}^K \vartheta(x/T_c). \end{aligned} \quad (15)$$

$$\begin{aligned}
I_{k'}^{u'}(t) &= \frac{1}{T_{MC}} \int_0^{T_{MC}} \sum_{n'=-\infty}^{\infty} X_{k',n'}^{u'}(nT_{MC} + t + t') c_n^u(t' + nT_{MC}) e^{-j2\pi f_k(t'+nT_{MC})} dt', \\
&= \frac{1}{T_{MC}} \int_0^{T_{MC}} \sum_{n'=-\infty}^{\infty} \psi_{k'}^{u'}(nT_{MC} + t + t') \sum_{p=1}^P G_{k',p}^{u'}(nT_{MC} + t + t') \epsilon_{k',p}^{u'}(nT_{MC} + t + t') b_{k',n'}^{u'} \\
&\quad c_{n'}^{u'}(nT_{MC} + t + t' - \tau_p^{u'}) e^{j2\pi f_{k'}(nT_{MC} + t + t' - \tau_p^{u'})} c_n^u(t' + nT_{MC}) e^{-j2\pi f_k(t'+nT_{MC})} dt', \\
&= \frac{1}{T_{MC}} \sum_{n'=-\infty}^{\infty} b_{k',n'}^{u'} \psi_{k'}^{u'}(nT_{MC}) \sum_{p=1}^P G_{k',p}^{u'}(nT_{MC}) \epsilon_{k',p}^{u'}(nT_{MC}) e^{j2\pi f_{k'}(t - \tau_p^{u'})} \\
&\quad \int_0^{T_{MC}} c_{n'}^{u'}(nT_{MC} + t + t' - \tau_p^{u'}) c_n^u(t' + nT_{MC}) e^{-j2\pi(f_{k'} - f_k)(t'+nT_{MC})} dt'.
\end{aligned} \tag{11}$$

$$\vartheta(x/T_c) = \begin{cases} 1 - \frac{\beta}{2} - \frac{x}{2} + \frac{3\beta}{4\pi} \sin\left(\frac{\pi x}{\beta}\right) + \left(\frac{\beta}{4} - \frac{x}{4}\right) \cos\left(\frac{\pi x}{\beta}\right) & \text{if } 0 \leq x \leq \min(\beta, 1 - \beta), \\ 1 - x & \text{if } \beta \leq x \leq 1 - \beta \text{ and } \beta < 0.5, \\ \frac{3}{4} - \frac{\beta}{4} - \frac{x}{4} + \frac{3\beta}{4\pi} \sin\left(\frac{\pi x}{\beta}\right) + \left(\frac{\beta}{4} - \frac{x}{4}\right) \cos\left(\frac{\pi x}{\beta}\right) + \frac{3\beta}{8\pi} \sin\left(\frac{\pi x}{\beta} - \frac{\pi}{\beta}\right) - \\ \left(\frac{x}{8} - \frac{1-\beta}{8}\right) \cos\left(\frac{\pi x}{\beta} - \frac{\pi}{\beta}\right) & \text{if } 1 - \beta \leq x \leq \beta \text{ and } \beta > 0.5, \\ \frac{3}{4} + \frac{\beta}{4} - \frac{3x}{4} + \frac{3\beta}{8L} \sin\left(\frac{\pi x}{\beta} - \frac{\pi}{\beta}\right) - \left(\frac{x}{8} - \frac{1-\beta}{8}\right) \cos\left(\frac{\pi x}{\beta} - \frac{\pi}{\beta}\right) & \text{if } \max(\beta, 1 - \beta) \leq x \leq 1, \\ \frac{1}{4} + \frac{\beta}{4} - \frac{x}{4} - \frac{3\beta}{8L} \sin\left(\frac{\pi x}{\beta} - \frac{\pi}{\beta}\right) - \left(\frac{1+\beta}{8} - \frac{x}{8}\right) \cos\left(\frac{\pi x}{\beta} - \frac{\pi}{\beta}\right) & \text{if } 1 \leq x \leq 1 + \beta, \\ 0 & \text{if } 1 + \beta \leq x. \end{cases} \tag{16}$$

Note that $\vartheta(x/T_c)$ represents the variance of the interference between subcarriers f_k and $f_{k'}$, multiplied by L . It is easy to obtain $\zeta(\beta) = (1 - \frac{\beta}{4})$. But we need to derive the integral with different frequency spacings to obtain $\vartheta(x/T_c)$ in Eq. (16). The normalized variance of the interference at the base-station antennas is:

$$\begin{aligned}
\text{Var}[I] &= \frac{1}{L} [(U - 1)(\zeta(\beta) + \chi(\beta)) + \frac{P-1}{P}(\zeta(\beta) + \chi(\beta))] \\
&\quad + \frac{1}{L} [U f_{out}(\zeta(\beta) + \chi(\beta))] + \sigma_N^2,
\end{aligned} \tag{17}$$

where f_{out} is the out-cell to in-cell interference ratio [11], $(U - 1)(\zeta(\beta) + \chi(\beta))/L$ is the normalized variance of the MAI ($u' \neq u$), $\frac{P-1}{PL}\zeta(\beta)$ is the normalized variance of the ICI ($k' \neq k$ and $u' = u$), $\frac{P-1}{PL}\chi(\beta)$ is the normalized variance of the ISI ($k' = k$ and $u' = u$), and $U f_{out}(\zeta(\beta) + \chi(\beta))/L$ is the normalized variance of the out-cell interference. Note that we assumed in the development of Eq. (17) an equal average power for all multipaths. Having obtained the variance of the interference, the average BER of a BPSK modulated MC-CDMA system communicating over perfectly estimated Rayleigh fading channels can be evaluated using Eq. (47) in [2]:

$$P_b = \frac{1}{\pi} \int_0^{\pi/2} \prod_{l=1}^{MP} \left(\frac{\sin^2 \theta}{\text{Var}[I]^{-1} + \sin^2 \theta} \right) d\theta. \tag{18}$$

4. NUMERICAL RESULTS

Fig. 2 gives us an insight into the interference behavior for different chip waveforms associated with different subcar-

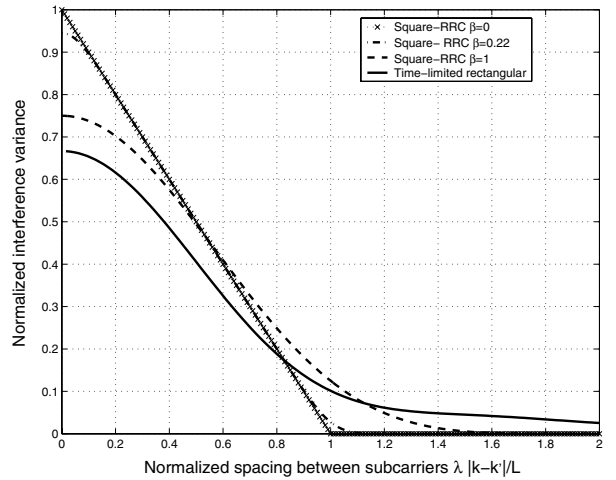


Fig. 2. Normalized interference variance of (16) versus the normalized spacing between subcarriers f_k and $f_{k'}$ with respect to the band-limited square-root RC and time-limited rectangular waveforms.

rier spacings. For all chip waveforms considered, we observe that the interference power decreases when increasing the absolute spacing value of $(|k - k'| \lambda / L)$. If we have $(|k - k'| \lambda / L) < 0.8$, which implies a small subcarrier spacing (i.e., DS-CDMA and MT-CDMA), a spreading sequence using a time-limited rectangular chip waveform generates the lowest interference power, while using a square-RRC with $\beta = 0$ results in the highest interference power. Hence, the performance evaluation without band-limitation filtering leads to an underestimation of the

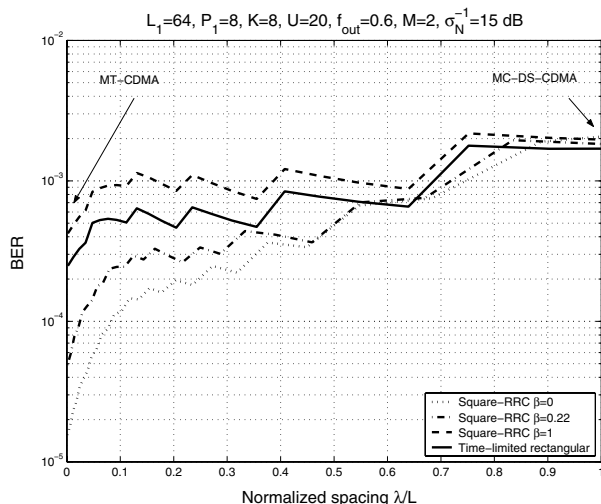


Fig. 3. BER versus the normalized subcarrier spacing $\frac{\lambda}{L}$ for an MC-CDMA system.

interference when the subcarriers are close. When increasing the spacing, we can observe that there exists a spacing range where the square-root RC (square RRC) chip waveforms outperform the rectangular chip waveform. The interference power at the point $(|k - k'| \lambda / L) = 1$ (i.e. MC-DS-CDMA) is 3 times lower with square-root RC with $\beta = 0.22$ than that with a rectangular chip waveform. Therefore, we can infer that in a MC-DS-CDMA system, band-limitation filtering reduces the inter-carrier interference.

The influence of the chip waveform and the normalized subcarrier spacing $\frac{\lambda}{L}$, on the average BER of the MC-CDMA system is shown in Fig. 3, where we assume that the receiver is capable of combining all the resolvable paths. The simulation parameters are listed at the top of Fig. 3. From the simulation results, we observe that for all the chip waveforms considered there exists an optimum value of λ , which will minimize the average BER. The optimum value is identical for all four types of chip waveforms and it is $\lambda = 1$. Hence the MT-CDMA achieves the best BER performance. Indeed, the BER improvement due to using longer spreading sequences and exploiting the frequency diversity is higher than the degradation caused by the inter-carrier interference. Moreover, for a given total system bandwidth, the square-RRC chip waveforms with $\beta = 1$ has less frequency diversity due to the reduced chip rate, while the chip waveforms with $\beta = 0$ allow the receiver to exploit path diversity and achieve better performance. We show here that if the receiver is capable of combining all the resolvable paths, the positive effect of frequency diversity is more significant than the negative effects of multipath and multi-carrier interference. Finally, we observe that when $\frac{\lambda}{L} = 1$, the MC-DS-CDMA system using any of the four chip waveforms performs nearly the same.

5. CONCLUSION

In summary, the generalized MC-CDMA system defined in [2] has been investigated in this paper by assuming that the spreading sequences use *band-limited* chip waveforms, namely, square-root raised cosine waveforms. The effects of the chip waveforms and the spacing between two adjacent subcarriers on the average bit error rate (BER) have been evaluated. The results show that for a given subcarrier spacing between two adjacent subcarriers, there exists a corresponding best choice of chip waveform. In addition, they suggest that MT-CDMA has the optimum spacing between subcarriers and achieves the best BER performance.

6. REFERENCES

- [1] S. Hata and R. Prasad, "Overview of multicarrier CDMA", *IEEE Commun. Mag.*, vol. 35, no. 12, pp. 126-133, December 1997.
- [2] Y. Lie-Liang and L. Hanzo, "Performance of generalized multicarrier DS-CDMA over Nakagami-m fading channels", *IEEE Transactions on Communications*, vol. 50, no. 6, pp. 956-966, June 2002.
- [3] Z. Guozhen and L. Cong, "Performance evaluation for band-limited DS-CDMA systems based on simplified improved Gaussian approximation", *IEEE Transactions on Communications*, vol. 51, no. 7, pp. 1204-1213, July 2003.
- [4] H. H. Nguyen and E. Shwedyk, "On error probabilities of DS-CDMA systems with arbitrary chip waveforms," *IEEE Commun. Lett.*, vol. 5, pp. 78-80, Mar. 2001.
- [5] Y. Lie-Liang and L. Hanzo, "Performance of generalized multicarrier DS-CDMA using various chip waveforms", *IEEE Transactions on Communications*, vol. 51, no. 5, pp. 748-752, May 2003.
- [6] L. Vandendorpe, "Multitone spread spectrum multiple access communications system in a multipath Rician fading channel", *IEEE Transactions on Vehicular Technology*, vol. 44, no. 2, pp. 327-337, May 1995.
- [7] Q.M. Rahman and A. B. Sesay, "Performance analysis of MT-CDMA system with diversity combining", *IEEE MILCOM 2001*, vol. 2, pp. 1360-1364.
- [8] H. H. Nguyen, "Effect of chip waveform shaping on the performance of multicarrier CDMA systems", *IEEE Transactions on Vehicular Technology*, vol. 54, no. 3, pp. 1022-1029, May 2005.
- [9] S. Kondo, and B. Milstein, "Performance of multicarrier DS CDMA systems", *IEEE Transactions on Communications*, vol. 44, no. 2, pp. 238-246, February 1996.
- [10] W.C. Jakes, et al, *Microwave Mobile communications*, New York: Wiley, 1974.
- [11] T.S. Rappaport, *Wireless communications: principles & practice*, Prentice Hall PTR 1999.